ISSN 2029-6991 / eISSN 2029-7009

VILNIUS TECH
Vilnius Gediminas Technical University

GEODESY and CARTOGRAPHY

2026
Volume 52
Issue 1
Pages 33–41
https://doi.org/10.3846/gac.2026.21948

UDC 528.21

MODELLING THE LOCAL GEOID OF EAST KALIMANTAN FROM COMBINATION OF AIRBORNE AND TERRESTRIAL GRAVITY DATA USING THE KTH METHOD

Sukma Nur OKTAVIA[1,2], Leni Sophia HELIANI[1]✉

[1]*Department of Geodetic Engineering, Faculty of Engineering, Gadjah Mada University, Yogyakarta, Indonesia*
[2]*Directorate of Geospatial Reference Systems, Geospatial Information Agency, Cibinong, Indonesia*

Article History:
- received 23 August 2024
- accepted 04 March 2026

Abstract. This research aims to determine the gravimetric geoid using the KTH method for East Kalimantan, where Indonesia's new capital city is located. The geoid of East Kalimantan was calculated from a combination of airborne gravity data, terrestrial gravity data, DTU17 for the sea area, anomalies of EGM2008 degree 2190, SRTM15+, and GGM from EGM2008 degree 360. The geoid modelling is performed using LSMSSOFT software with a grid interval of 0.01˚. The evaluation of capsize variations includes 14 variations: 0.1˚, 0.2˚, 0.3˚, 0.4˚, 0.5˚, 0.6˚, 0.7˚, 0.8˚, 0.9˚, 1˚, 1.2˚, 1.3˚, 1.5˚, and 2˚. The KTH geoid was evaluated using 264 GNSS-Levelling data points. The best accuracy was obtained at a capsize of 0.6˚ with a standard deviation value of 0.0532 m. The accuracy of the geoid model after shifting to the tidal benchmark (BM) is 0.0526 m. A comparison with the recent national geoid model of INAGEOID2020 v.2 obtained using the Remove-Restore method, which has a standard deviation of 0.0588 m, shows that the accuracy of the KTH method geoid model is higher, with a precision improvement of 0.0062 m.

Keywords: geoid, airbone, terrestrial, gravity, KTH, East Kalimantan.

✉Corresponding author. E-mail: ***lheliani@ugm.ac.id***

1. Introduction

Mapping survey activities are growing rapidly, along with developments in mapping using Global Navigation Satellite System (GNSS) technology. Positioning with GNSS can be done quickly and accurately to produce a 3D position (Ly et al., 2021). Although GNSS technology can provide accurate positions, the resulting height is geometric with no physical meaning. Geoid undulations are required to convert geometric height to physical or orthometric height. Geoid undulations represent the relationship between the physical and geometric shapes of the Earth (Featherstone & Kuhn, 2006). Geoid undulations can be obtained by modeling the geoid in a certain area. The geoid is an equipotential surface that coincides with the undisturbed mean sea level (Hofmann-Wellenhof & Moritz, 2005).

Geoid modeling can be done geometrically using GNSS-Levelling data and gravimetrically using gravity data (Sylvester et al., 2018). A precise gravimetric geoid is required to obtain accurate heights. Several factors influence the accuracy of the geoid model, including the accuracy and density of gravity data, DEM accuracy, GNSS-Levelling data accuracy, and the calculation method used (Jalal et al., 2019).

Gravimetric geoid modeling can be calculated using the Stokes and Hotine approaches (Sakil et al., 2021). The Stokes approach uses free-air gravity anomalies as input data, while the Hotine approach uses gravity disturbance data (Işık et al., 2021). The Stokes function approach can be completed using the Remove Compute Restore (RCR) method, which involves removing the influence of topography and GGM from gravity data (remove), then adding it back to the geoid undulation calculation (restore) (Sansò & Sideris, 2013).

The weakness of the Stokes formula with the RCR method is that it requires all gravity data from the global geopotential model. This causes truncation errors to occur, reducing some of the gravity anomaly signals (Abbak et al., 2012). The Royal Institute of Technology (KTH) developed the Least Squares Modification of the Stokes Formula method, or the KTH method. In the KTH method, the integral area is limited around the calculation point only to minimize errors in using GGM. With the KTH method, the contribution of gravity anomalies at distant points, considered as truncation errors, is overcome by applying a modification of the Stokes function (Sjöberg, 2003).

The process of calculating the KTH geoid model involves several stages. The first step is to determine the

approximate geoid undulation value. This value is then augmented with four additive corrections: topographic correction, downward continuation correction, atmospheric correction, and ellipsoid correction (Abdalla & Tenzer, 2011). The GGM coefficient and gravity data gridding influence the approximate undulation calculation. One key parameter affecting the results of KTH geoid modeling is the capsize value used (Pa'suya et al., 2021). Therefore, capsize evaluation is crucial to achieve optimal accuracy in the KTH geoid model.

The KTH method has been widely used in various countries. Countries that use the KTH method for geoid modeling include Malaysia (Pa'suya et al., 2021), Turkey (Yildiz et al., 2021), and Bosnia (Krdžalić & Abbak, 2023). As geoid modeling using the KTH method was developed in various countries, KTH method calculation software, namely LSMSSOFT, was developed (Abbak & Ustun, 2015). The KTH method produces higher geoid model accuracy in mountainous areas than the RCR method (Abbak et al., 2012). The KTH geoid model has higher accuracy in flat areas but is not significantly different from the RCR method (Wu et al., 2020). Although the KTH method has been tested in various countries for geoid modeling, geoid modeling in Indonesia generally uses the RCR method. The geoid modeling of Kalimantan in the INAGEOID2020 v.2 national geoid model was also calculated using the RCR method with an accuracy of around 5–28 cm (Center for Geodesy and Geodynamics Control Network BIG, 2023). Based on this, it is necessary to evaluate the KTH method for geoid modeling in Indonesia.

This research was conducted to model the gravimetric geoid using the KTH method for the East Kalimantan, where the new Indonesian capital city, named Nusantara, is located. The data combination uses the latest airborne and terrestrial gravity data from 2021 and 2022. To obtain optimal accuracy, 14 capsize variations were evaluated. The accuracy of the geoid model is obtained by comparing the geometric geoid undulation values at 264 GNSS-Levelling points.

2. Data and methodology

2.1. Data and location

This research was carried out with gravimetric geoid modeling using the KTH method in the East Kalimantan region, covering an area from 2.4˚ S to 3.5˚ N and from 113˚ E to 119˚ E. The research area includes the entire land administrative boundaries of East Kalimantan and parts of the surrounding sea. The research area coverage is shown in Figure 1.

The data used in this research are as follows:

1. Airborne gravity data

The airborne data is secondary data from the Geospatial Information Agency (BIG). The airborne gravity data consists of two sets, the 2021 and 2022 datasets. Airborne gravity measurements were taken using the GT-2A gravimeter. The average flight path interval is 16 km, with

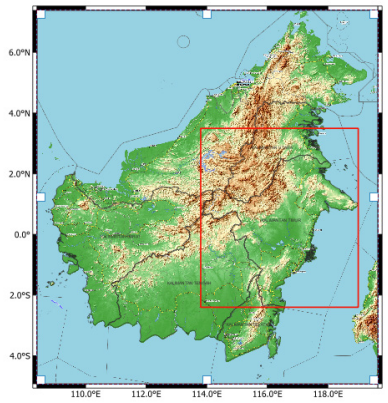

Figure 1. Coverage of the research area (source: author's own work)

an average flight height of 3200 m above the ellipsoid surface. The airborne data has been processed with downward continuation so that the values are referenced to the ellipsoid's surface. The airborne gravity data covers all land and sea areas up to 20 km from the coastline.

2. Terrestrial gravity data

The terrestrial gravity data used is secondary data measured by BIG in 2021 using a CG-5 gravimeter with an instrument accuracy of 1 μGal. The dataset consists of 88 points with a data interval of 5 km. The terrestrial gravity data measurement path forms a loop from the reference point, returning to the reference point on the same day. The main reference is the absolute gravity from the GBU pillar of order 0 GBU.025 at the Sepinggang Airport Meteorological Station, with a value of 978039.87967 mgal. The daily drift value meets the requirement of ≤ 0.1 mgal.

3. DTU 17

DTU 17 data was obtained from the link https://ftp.space.dtu.dk/pub/DTU17/1_MIN/. This data is used to fill the gaps in gravity data in marine areas. DTU data selection is carried out by a buffer process of 8 km from the outermost airborne gravity data.

4. EGM2008 anomaly data (degree 2190)

The northwestern part of the research area is part

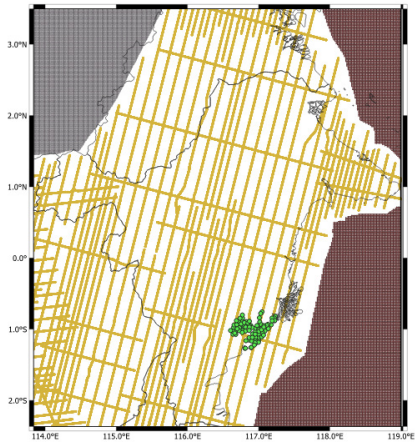

Figure 2. Combination of airborne (yellow), terrestrial (green), DTU17 gravity data (red), and the EGM2008 degree 2190 anomaly (black) (source: author's own work)

of the plains region (Malaysia), resulting in a data gap in that region. To fill the data gaps in the land area, the EGM2008 degree 2190 anomaly data is used (Figure 2).

5. Digital Terrain Model (DTM)

DTM data uses Shuttle Radar Topography Mission (SRTM)15+ data downloaded from the link https://topex.ucsd.edu/cgi-bin/get_srtm15.cgi. DTM data is used to calculate topographic corrections and downward continuation corrections (Pa'suya et al., 2021).

6. Global Geopotential Model (GGM)

In this research, the global geopotential model will first be evaluated for geometric undulations at GNSS-levelling points. The GGM data evaluated consists of 5 gravity satellite GGMs and 1 hybrid GGM. The GGM gravity satellites used are GO_CONS_GCF_2_TIM_R6, ITU_GGC16I, GGT_R1, GO_CONS_GCF_2_SPW_R5, and GO_CONS_GCF_2_DIR_R6, each at degree 240. The hybrid GGM uses EGM2008 at degree 360.

7. GNSS-Levelling data

GNSS-Levelling data totaling 264 points is used to calculate geometric geoid undulations. GNSS-Levelling data was obtained from BIG and acquired in 2020. Geodetic GNSS observations obtained geodetic coordinates carried out for 12 hours at temporary points and 36 hours at permanent points with obstruction <15˚. GNSS data coordinates meet the condition that the coordinate difference between processing two baselines is less than 5 cm for the horizontal component and 10 cm for the vertical component. Accurate leveling measurements consist of sub-sections and sections. Measurements were carried out BFFB (B: Backward and F: Forward) with a closing error tolerance of 8 mm √d.

8. Tidal station benchmark data

The resulting geoid model uses tidal station data for the shifting process. This data was obtained from the official SRGI website via the link https://srgi.big.go.id/map/jkg-active (Center for Geodesy and Geodynamics Control Network BIG, 2023). The tidal BMs used in the shifting step consist of Tarakan and Balikpapan stations. Tidal BM information is presented in Table 1.

The distribution of GNSS-Levelling and tidal BM data is shown in Figure 3.

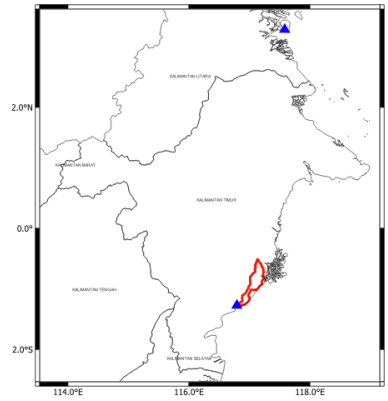

Figure 3. Distribution of GNSS-Levelling data (red) and Tidal BM data (blue) (source: author's own work)

3. Methodology

Geoid modeling using the KTH method employs LSMSSOFT software with a grid interval of 0.01˚. The KTH geoid model calculation uses airborne, terrestrial, DTU17, EGM2008, and SRTM15+ gravity data. The capsize evaluation includes 14 variations: 0.1˚, 0.2˚, 0.3˚, 0.4˚, 0.5˚, 0.6˚, 0.7˚, 0.8˚, 0.9˚, 1˚, 1.2˚, 1.3˚, 1.5˚, and 2˚. Shifting the geoid model is carried out using 2 tidal BM points. The accuracy of the KTH geoid model was obtained by comparing it to geometric undulations from GNSS-Levelling measurements at 264 validation control points.

The research stages generally include data preparation, geoid modeling, shifting, and geoid validation. The preparation stage includes data and software preparation. The software used includes:

a. QGIS and Global Mapper15 for gridding DTM data and gravity data;
b. GEOEGM and GEOIP Sub Programs on GRAVSOFT for GGM data evaluation and geoid validation;
c. LSMSSOFT for geoid modeling using the KTH method;
d. GMT 5 for data visualization.

The geoid modeling stage, conducted with the LSMSSOFT program, is a comprehensive process that produces geoid undulation values, approximate undulation, and additive corrections. The required input data includes gridded SRTM15+ data, gridded free-air anomaly data, and GGM data.

Gravity anomaly data around the research location is needed for the calculations. In the KTH method, the data area and target area are defined. The target area is the coverage of the research area, while the data area is the region around the research location that influences the undulation calculation. The data coverage area is greater than the target area by at least 1˚ (Krdžalić & Abbak, 2023). In this study, the data area limits were 3.4˚ South Latitude to 4.5˚ North Latitude and 112.8˚ East Longitude to 120˚ East Longitude. In the data area, gravity data is filled using the anomalyfill subprogram with input anomaly data EGM2008 degree 2190.

To obtain the optimal combination of GGM and capsize in KTH geoid modeling, an evaluation was carried

Table 1. Tidal BM height information (source: Center for Geodesy and Geodynamics Control Network BIG, 2023)

Station	Code	Latitude (˚)	Longitude (˚)	h (m)	H (m)	N (m)
Tarakan	0TRK	3.2838	117.596	60.173	3.759	56.414
Balikpapan	0BLP	–1.2725	116.806	57.693	4.093	53.601

out on 1) 5 gravity satellite GGMs and 1 hybrid GGM, and 2) 14 capsize variations. GGM evaluation was carried out by calculating the undulation value of 6 GGMs using GEOEGM with an interval of 0.01˚. Interpolation of GGM undulations at GNSS-Levelling points was performed using the GEOIP program. The standard deviation is calculated from the difference between the GGM undulations and the geometric undulations at the GNSS-Levelling points. The smallest standard deviation is used as the optimal GGM.

The results of the geoid calculation were shifted to tidal BM. Shifting aims to bring the geoid undulation value closer to the mean sea level and maintain the geoid pattern. This stage is carried out using the GEOIP subprogram on GRAVSOFT. The accuracy of the geoid model is obtained by comparing it with the geometric geoid undulation values at 264 points using the GEOIP subprogram.

The KTH method modifies the Stokes equation by calculating the approximate geoid undulation value and adding the additive correction value. Geoid undulations are calculated using the Stokes function in Equation (1).

$$N = \frac{R}{4\pi\gamma_{\sigma}} S(\Psi)\Delta g d\sigma. \quad (1)$$

The KTH method modifies the Stokes equation by calculating the approximate geoid undulation value and adding the additive correction value. The determination of the approximate geoid undulation ($\tilde{N}$) in Equation (2) is calculated based on the modification parameters b_n and S_n in Equation (3).

$$\tilde{N} = \frac{R}{4\pi\gamma_{\sigma_0}} S^L(\Psi)\Delta g d\sigma + \frac{R}{2\gamma}\sum_{n=2}^{M} b_n \Delta g_n^{GGM}. \quad (2)$$

In this case, M is the maximum degree of *GGM*, Δg_n^{GGM} is the *GGM* anomaly, and $S^L(\psi)$ is a modification of the Stokes function, which is described in Equation (3).

$$S^L(\psi) = \sum_{n=2}^{\infty} \frac{2n+1}{n-1} P_n(\cos\psi) - \sum_{n=2}^{L} \frac{2n+1}{2} S_n P_n(\cos\psi). \quad (3)$$

The next crucial step in our research is adding the approximate geoid value ($\hat{N}$) with four additive corrections to derive the geoid undulation value. The geoid undulation ($\hat{N}$) in the KTH method is calculated using the Equation (4).

$$\hat{N} = \tilde{N} + \delta N_{comb}^{Top} + \delta N_{DWC} + \delta N_{comb}^{Atm} + \delta N_{ell}. \quad (4)$$

The topographic correction is calculated using Equation (5).

$$\delta N_{comb}^{Top} = \delta N_{dir} + \delta N_{indir}^{Top} = -\frac{2\pi G\rho}{\gamma} H^2 \left(1 + \frac{2H}{3R}\right). \quad (5)$$

G is the gravitational constant, ρ is the topographic mass density, and H is the orthometric height. The downward continuation correction is calculated using Equations (6) to (9):

$$\delta N_{DWC} = \delta N_{dwc}^{(1)} + \delta N_{dwc}^{L1,Far} + \delta N_{dwc}^{L2}, \quad (6)$$

where

$$\delta N_{dwc}^{(1)} = \frac{\Delta g_p}{\gamma} H_P + 3\frac{\tilde{N}}{r_p} H_P - \frac{1}{2\gamma}\frac{\partial \Delta g}{\partial r}\Big|_P H_P^2 \quad (7)$$

and

$$\delta N_{dwc}^{L1,Far} = \frac{R}{2\gamma}\sum_{n=2}^{M} b_n \left[\left(\frac{R}{r_p}\right)^{n+2} - 1\right]\Delta g_n \quad (8)$$

also

$$\delta N_{dwc}^{L2} = \frac{R}{4\pi\gamma_{\sigma_0}} S^L(\Psi)\left[\frac{\partial \Delta g}{\partial r}\Big|_P \left(H_P - H_Q\right)\right] d\sigma_0. \quad (9)$$

The atmospheric correction is calculated using Equation (10).

$$\delta N_{comb}^{Atm} = -\frac{GR\rho^a}{\gamma_{\sigma_0}} S^L(\Psi) H d\sigma_0. \quad (10)$$

The ellipsoid correction is calculated using Equation (11).

$$\delta N_{ell} \approx \left[\left(0.0036 - 0.0109\sin^2\varphi\right)\Delta g + 0.005050\tilde{N}\cos^2\varphi\right] Q_0^L. \quad (11)$$

4. Results and discussion

4.1. Gridded free-air gravity anomaly

The main input data for geoid modeling is free-air anomaly data in grid format with intervals of 0.01° × 0.01°. The gravity data gridding procedure is carried out on the Bouguer plane by first converting the free-air anomaly into a simple Bouguer anomaly. Simple Bouguer anomalies are more optimal for gridding data because they are smoother and not affected by topography (Krdžalić & Abbak, 2023). The interpolation method used is nearest neighbor. The gridded simple Bouguer anomaly is then converted back into a free-air anomaly. The gridding procedure requires SRTM15+ data that has been gridded with an interval of 0.01°.

Figure 4 shows that SRTM15+ data has variations in height ranging from –5000 m to 2500 m. The topographic pattern of SRTM15+ indicates that the central part of East Kalimantan is flat with a height above 1500 m, while other parts of the region are relatively flat. The free-air anomaly pattern is identical to the EGM2008 degree 2190 anomaly pattern. Most of the free-air anomaly values for East Kalimantan range from 75 mgal to 150 mgal, with only the central part having higher values, specifically 225 mgal to 255 mgal. This anomaly pattern follows the topographic pattern, where inland areas have higher values, represented by the color green with a range from 75 mgal to 250 mgal, while in the sea, the values tend to be lower, shown in light blue to purple, which is close to 0 mgal to –90 mgal. This is because the density of seawater is lower compared to land areas.

A comparison of the three anomaly data sets in Table 2 shows that the combined anomaly with the airborne

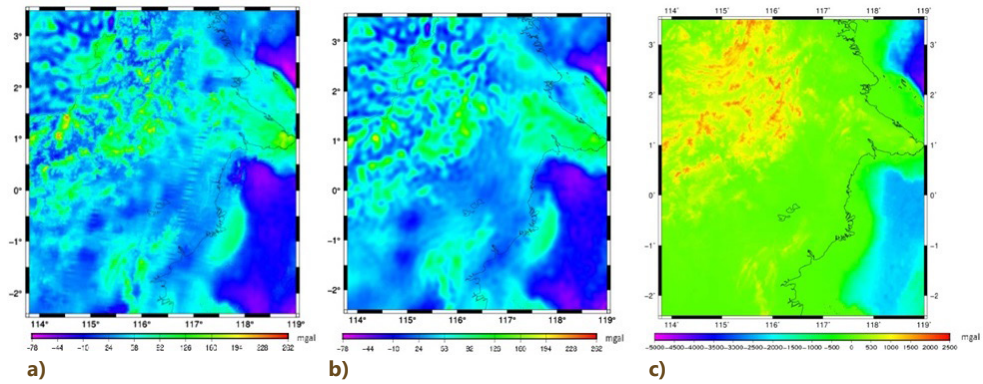

Figure 4. Gridded data: a) free-air anomaly; b) EGM2008 degree 2190 anomaly; c) topography (source: author's own work)

anomaly has a wider range and more varied values. Additionally, the combined anomaly for EGM 2008 has relatively similar minimum (min), maximum (max), mean, and standard deviation (STD) values.

Table 2. Free-air anomaly statistics (source: author's own work)

Anomaly	Min (mgal)	Max (mgal)	Mean (mgal)	STD (mgal)
Airborne	–37.740	237.311	51.257	28.595
Combination	–78.635	261.144	42.581	36.083
EGM2008	–76.427	210.842	41.218	34.554

4.2. Evaluation of global geopotential models

The GGM evaluation aims to identify the best GGM to be used as a long-wave component in geoid modeling. This evaluation is conducted by comparing the undulation value of each GGM with the geometric geoid undulation at the GNSS-Levelling points. The GGM with the smallest standard deviation is considered the best and is used for geoid model calculations. The GGM undulation calculation uses GEOEGM with an interval of 0.01˚ × 0.01˚. Six GGMs were evaluated, consisting of five gravity satellite GGMs and one hybrid GGM. The gravity satellite GGMs include GO_CONS_GCF_2_TIM_R6, ITU_GGC16I, GGT_R1, GO_CONS_GCF_2_SPW_R5, and GO_CONS_GCF_2_DIR_R6, each at degree 240. The hybrid GGM used is EGM2008 at degree 360. The comparison of GGM undulations with geometric undulations is shown in Table 3.

The gravity satellite GGM with the smallest standard deviation is SPW_R5, with a value of 0.152 m. Overall, the smallest standard deviation was obtained from EGM2008 at degree 360, with a value of 0.088 m. EGM2008 produces better accuracy than the gravity satellite GGMs because it combines surface and terrestrial data. Therefore, the next stage of the GGM used is EGM2008 at degree 360. Figure 5 visualizes the standard deviation comparison for each GGM.

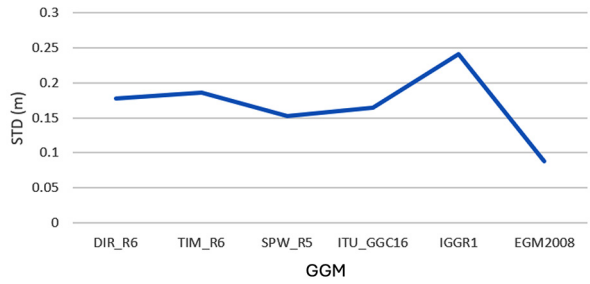

Figure 5. Visualization of the standard deviation comparison for each GGM (source: author's own work)

4.3. Evaluate capsize

Determining parameters when modeling geoids affects the accuracy of the resulting geoid model. The KTH method can only be applied to a limited degree of capsize, but there are no specific provisions for the use of capsize (Sjöberg, 2003). In this study, capsize evaluation was carried out on 14 variations to obtain optimal capsize parameters. The capsize variation with the smallest standard deviation represents the best model. The standard deviation value is obtained from the difference between the geometric geoid undulations. Capsize variations are 0.1˚, 0.2˚, 0.3˚, 0.4˚, 0.5˚, 0.6˚, 0.7˚, 0.8˚, 0.9˚, 1˚, 1.2˚, 1.3˚, 1.5˚, and 2˚. Statistics for each capsize are shown in Table 4.

Table 3. Comparison of GGM undulations with geometric undulations (source: author's own work)

GGM	DIR_R6	TIM_R6	SPW_R5	ITU_GGC16	IGGR1	EGM2008 (hybrid)
Degree	240	240	240	240	240	360
Min (m)	0.736	0.689	0.825	0.751	0.368	0.990
Max (m)	1.387	1.373	1.420	1.377	1.228	1.586
Mean (m)	1.061	1.033	1.127	1.072	0.804	1.301
STD (m)	0.177	0.186	0.152	0.165	0.241	0.088

Table 4. Geoid model accuracy statistics based on capsize (source: author's own work)

Capsize	0.1°	0.2°	0.3°	0.4°	0.5°	0.6°	0.7°	0.8°	0.9°	1°	1.2°	1.3°	1.5°	2°
Min (m)	0.153	0.187	0.201	0.21	0.230	0.248	0.248	0.241	0.236	0.219	0.161	0.147	0.164	0.367
Max (m)	0.609	0.608	0.617	0.629	0.638	0.645	0.647	0.649	0.654	0.658	0.638	0.625	0.669	0.838
Mean (m)	0.423	0.430	0.442	0.454	0.466	0.474	0.478	0.476	0.472	0.466	0.446	0.437	0.442	0.604
STD (m)	0.058	0.054	0.054	0.055	0.054	0.053	0.054	0.054	0.054	0.054	0.058	0.065	0.091	0.088

Based on Table 4, the smallest standard deviation value obtained from a capsize of 0.6˚ is 0.053 m, with a value range of 0.248 m to 0.645 m and an average of 0.474 m. In the next stage, the KTH geoid model is used with a capsize of 0.6˚. The size of the capsize value does not correlate with the size of the standard deviation value (Figure 6).

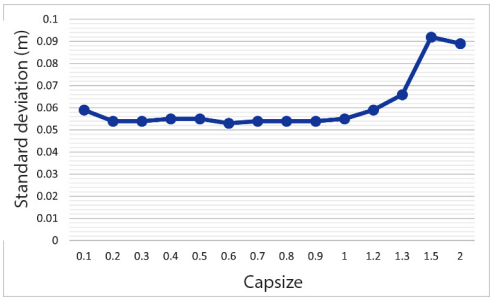

Figure 6. The comparison graph of standard deviation values for several capsize variations (source: author's own work)

4.4. Additive correction

Additive correction consists of topographic correction, atmospheric correction, downward continuation correction, and ellipsoid correction, as shown in Figure 7.

Topographic correction is calculated using Equation (5), where the H value is the height from SRTM15+ data. Topographic correction shows greater values in land areas than in sea areas. Atmospheric correction and ellipsoid correction show relatively small values, with atmospheric correction values ranging from –1.2 mm to 2.3 mm and ellipsoid correction values ranging from –2.3 mm to 1 mm. The highest atmospheric correction values are found in the northern sea area. The downward continuation correction values range from 0.07 m to 0.5 m, with higher values in Central East Kalimantan, where topography is more varied.

In general, based on Abbak et al. (2012), Wu et al. (2020), and Krdžalić and Abbak (2023), atmospheric and

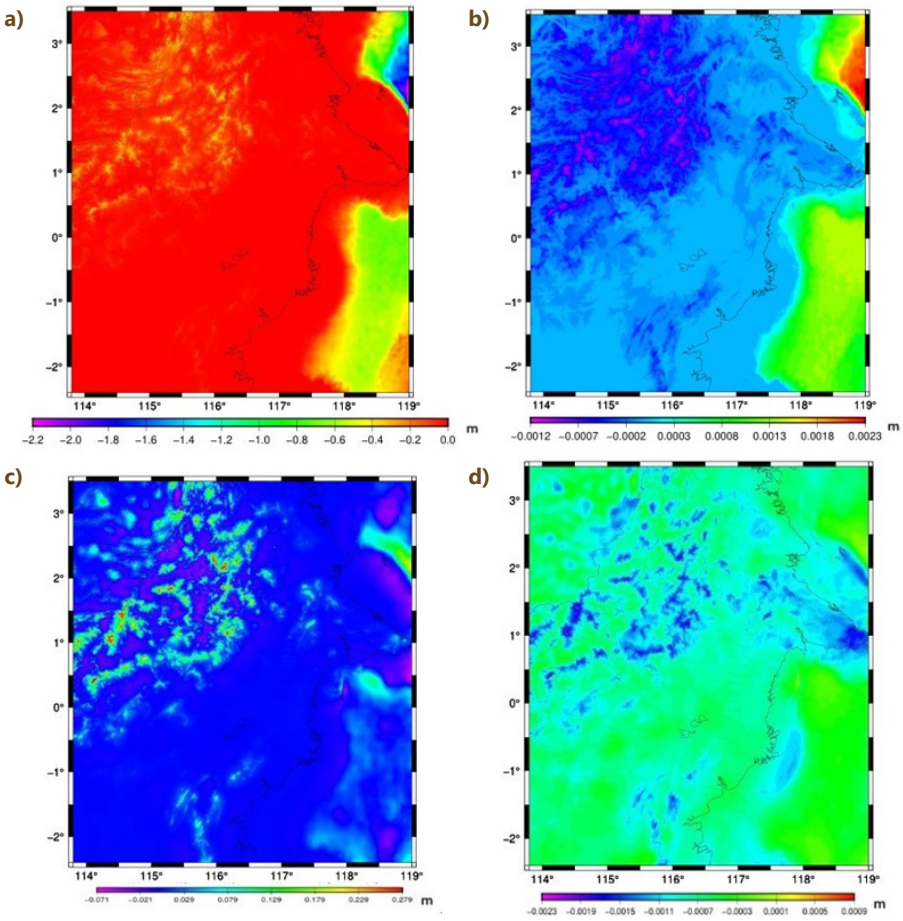

Figure 7. Additive correction: a) topographic correction; b) atmospheric correction; c) downward continuation correction; d) ellipsoid correction (source: author's own work)

ellipsoid correction values are only fractions of a millimetre, while topographic and downward continuation corrections have a more dominant influence (Table 5).

Table 5. Additive correction values (source: author's own work)

Correction	top	atm	dwc	ell
Min (m)	–2.218	–0.0012	0.5234	–0.0023
Max (m)	0	0.0025	–0.0711	0.0010

The summation of the approximate geoid undulations with four additive corrections produces the geoid undulations. Based on Table 6, adding additive corrections will reduce the range (minimum and maximum values), and on average, there is an increase of 0.094 meters in geoid undulations. This shows that geoid modeling with additive corrections will produce a smoother geoid model (Wu et al., 2020).

Table 6. Statistics of geoid undulations (source: author's own work)

Undulation (N)	Approximate geoid	Approximate geoid + additive correction
Min (m)	43.766	43.770
Max (m)	59.957	59.950
Mean (m)	53.190	53.284

5. KTH geoid model

The geoid model is calculated using the KTH method based on Equation (4). The geoid undulation accuracy test at 264 GNSS-Levelling points produced the most accurate value for the local East Kalimantan geoid gravimetric undulation, obtained by GGM EGM2008 degree 360 with a capsize of 0.6˚, namely 0.0532 m (Table 7). The next stage involves applying a geoid model bias correction, known as shifting. Shifting the geoid model aims to bring the gravimetric geoid undulation values closer to the geometric geoid undulation values from the tidal BM. The shifting calculation is performed by correcting the amount of bias obtained from the average value of the difference between the gravimetric and geometric undulations at the tidal BM points and applying this correction to the overall gravimetric undulation values. The geoid model bias correction in this study obtained a value of 0.491 m. The accuracy of the geoid model after shifting resulted in a standard deviation of 0.0526 m.

Table 7. Accuracy of the geoid model before shifting and after shifting (source: author's own work)

Accuracy geoid model	Before shifting	After shifting
Min (m)	0.2476	–0.2434
Max (m)	0.6450	0.1540
Mean (m)	0.4734	–0.0176
STD (m)	0.0532	0.0526

The difference in accuracy of the geoid model before and after shifting is 0.0006 m. Shifting does not significantly affect the accuracy of the geoid model; however, it is used to bring the gravimetric geoid undulation value closer to the mean sea level and maintain the pattern of the gravimetric geoid. The resulting gravimetric undulation values or local geoid models have undergone bias correction. Figure 8 shows the geoid model visualization.

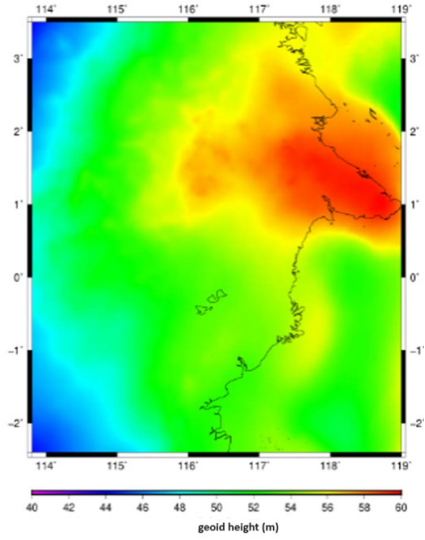

Figure 8. East Kalimantan KTH gravimetric geoid model (source: author's own work)

Overall, the geoid values of East Kalimantan exhibit a higher pattern from west to east, particularly in the northeast. The undulation values range from –0.2434 m to 0.1540 m. According to the Geospatial Information Agency, the INAGEOID2020 v2 national geoid model has an accuracy of 0.0588 m for the East Kalimantan region. This shows that the KTH method produces a higher geoid model accuracy with an improvement of 0.0062 m.

Figure 9a shows the difference between INAGEOID2020 v2 undulations and KTH undulations. The difference in undulation values ranges from –1.2 m to 2.2 m, with an average difference of 0.39 m. The undulation difference pattern aligns with the topographic pattern in Figure 9b. In areas with high topography, the undulation difference becomes greater, reaching up to 2.2 m. These results are consistent with research conducted by (Abbak et al., 2012), which concluded that there are significant differences between the KTH and RCR geoid models in the mountainous regions of Turkey. In high topographic areas, the geoid model results are influenced by various factors, including topographic mass density. Geoid model calculations involving mass density can improve geoid models in high topographic areas (Abbak, 2020).

Table 8 shows the difference between the geometric and gravimetric geoids from the KTH method, INAGEOID2020 v2, and the RCR method. The average difference between the geometric geoid and the KTH model is 0.0176 m, while for INAGEOID2020 v2 it is 0.0200 m.

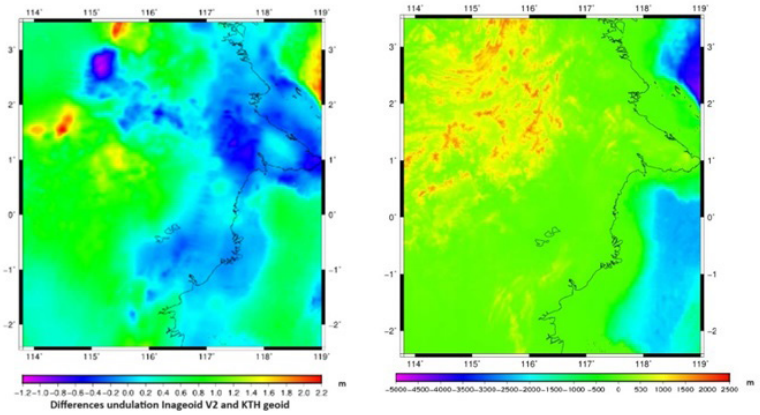

Figure 9. Difference in undulation: a) INAGEOID2020 v2 and KTH; b) topography (source: author's own work)

Table 8. Accuracy comparison between the KTH geoid model and INAGEOID2020 v2 (source: author's own work)

Geoid model	KTH	INAGEOID2020 v2
Min (m)	–0.2434	–0.1962
Max (m)	0.1540	0.2065
Mean (m)	–0.0176	0.0200
STD (m)	0.0526	0.0588

The difference values at each validation control point are shown in Figure 10. The pattern of differences in geometric and gravimetric undulations between the two models is almost the same at each validation control point. However, the INAGEOID2020 v2 model shows a greater difference in undulations compared to the KTH model.

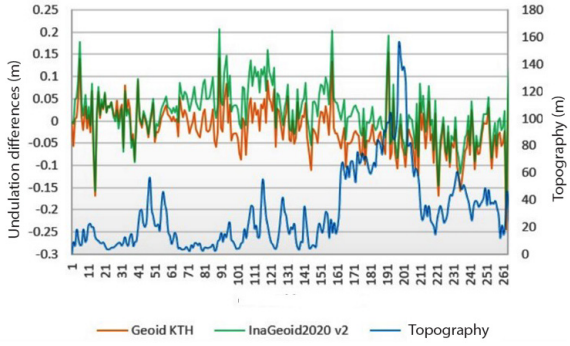

Figure 10. The difference between gravimetric undulations and geometric undulations, and the elevation of the East Kalimantan validation control points (source: author's own work)

6. Conclusions

Modelling the geoid using the KTH method produces approximate undulation values and four additive corrections. The topographic and downward continuation corrections contribute more significantly to the undulation values, while the ellipsoid and atmospheric corrections are only in the sub-millimetre range. Selecting the right MGG and capsize influences the resulting undulation value. Evaluation of several MGGs shows that the smallest standard deviation of the difference between MGG undulations and geometric undulations is obtained from EGM2008. The evaluation of 14 capsize variations identified an optimal capsize of 0.6˚ with a standard deviation of the geoid model of 0.0532 m. Shifting of the two tidal BMs of Tarakan and Balikpapan aims to bring the geoid undulation value closer to the mean sea level. The geoid model accuracy test compared the geometric geoid undulations from GNSS-Levelling data of 264 points. The test results showed that the accuracy of the geoid model after shifting was 0.0526 m. A comparison of the accuracy of INAGEOID2020 v2, with a standard deviation of 0.0588 m, shows that using the KTH method in the East Kalimantan region can increase the accuracy of the geoid model of 0.0062 m.

Acknowledgements

We gratefully acknowledge the Badan Informasi Geospasial for providing the airborne and terrestrial gravity datasets utilized in this study. Our sincere thanks also go to Abbak R. A. for access to the LSMSSOFT software. This research was undertaken within the framework of the Rekognisi Tugas Akhir (RTA) Grant Program, whose support is deeply appreciated.

References

Abbak, R. A. (2020). Effect of a high-resolution global crustal model on gravimetric geoid determination: A case study in a mountainous region. *Studia Geophysica et Geodaetica*, *64*(4), 436–451. https://doi.org/10.1007/s11200-020-1023-z

Abbak, R. A., Erol, B., & Ustun, A. (2012). Comparison of the KTH and remove–compute–restore techniques to geoid modelling in a mountainous area. *Computers & Geosciences*, *48*, 31–40. https://doi.org/10.1016/j.cageo.2012.05.019

Abbak, R. A., & Ustun, A. (2015). A software package for computing a regional gravimetric geoid model by the KTH method. *Earth Science Informatics*, *8*(1), 255–265. https://doi.org/10.1007/s12145-014-0149-3

Abdalla, A., & Tenzer, R. (2011). The evaluation of the New Zealand's geoid model using the KTH method. *Geodesy and Cartography*, *37*(1), 5–14. https://doi.org/10.3846/13921541.2011.558326

Center for Geodesy and Geodynamics Control Network BIG. (2023). *Sistem referensi geospasial Indonesia*. https://srgi.big.go.id/page/geoid-model, https://srgi.big.go.id/map/jkg-active

Featherstone, W. E., & Kuhn, M. (2006). Height systems and vertical datums: A review in the Australian context. *Journal of Spatial Science*, *51*(1), 21–41. https://doi.org/10.1080/14498596.2006.9635062

Hofmann-Wellenhof, B., & Moritz, H. (2005). *Physical geodesy*. Springer. https://doi.org/10.1007/b139113

Işık, M. S., Erol, B., Erol, S., & Sakil, F. F. (2021). High-resolution geoid modeling using least squares modification of Stokes and Hotine formulas in Colorado. *Journal of Geodesy*, *95*(5), 1–19. https://doi.org/10.1007/S00190-021-01501-z

Jalal, S. J., Musa, T. A., Md Din, A. H., Wan Aris, W. A., Shen, W., & Pa'suya, M. F. (2019). Influencing factors on the accuracy of local geoid model. *Geodesy and Geodynamics*, *10*(6), 439–445. https://doi.org/10.1016/j.geog.2019.07.003

Krdžalić, D., & Abbak, R. A. (2023). A precise geoid model of Bosnia and Herzegovina by the KTH method and its validation. *Survey Review*, *55*(393), 513–523. https://doi.org/10.1080/00396265.2022.2163361

Ly, C. A. T., Diene, J. M. L., Diouf, D., Ba, A., Ly, C. A. T., Diene, J. M. L., Diouf, D., & Ba, A. (2021). GNSS technology's contribution to topography: Evaluative study of gaps between methods topographies. *Journal of Geographic Information System*, *13*(3), 340–352. https://doi.org/10.4236/jgis.2021.133019

Pa'suya, M. F., Din, A. H. M., Yusoff, M. Y. M., Abbak, R. A., & Hamden, M. H. (2021). Refinement of gravimetric geoid model by incorporating terrestrial, marine, and airborne gravity using KTH method. *Arabian Journal of Geosciences*, *14*(19), 1–19. https://doi.org/10.1007/S12517-021-08247-0

Sakil, F. F., Erol, S., Ellmann, A., & Erol, B. (2021). Geoid modeling by the least squares modification of Hotine's and Stokes' formulae using non-gridded gravity data. *Computers & Geosciences*, *156*, Article 104909. https://doi.org/10.1016/j.cageo.2021.104909

Sansò, F., & Sideris, M. G. (Eds.). (2013). *Geoid determination* (Vol. 110). Springer. https://doi.org/10.1007/978-3-540-74700-0

Sjöberg, L. E. (2003). A general model for modifying Stokes' formula and its least-squares solution. *Journal of Geodesy*, *77*(7–8), 459–464. https://doi.org/10.1007/S00190-003-0346-1

Sylvester, E., Olujimi, O., Sunday, O., & Candidate, P. D. (2018). Procedure for the determination of local gravimetric-geometric geoid model. *International Journal of Advances in Scientific Research and Engineering* (*IJASRE*), *4*(8), 206–214. https://doi.org/10.31695/IJASRE.2018.32858

Wu, Q., Wang, H., Wang, B., Chen, S., & Li, H. (2020). Performance comparison of geoid refinement between XGM2016 and EGM2008 based on the KTH and RCR methods: Jilin Province, China. *Remote Sensing*, *12*(2), Article 324. https://doi.org/10.3390/rs12020324

Yildiz, H., Simav, M., Sezen, E., Akpinar, I., Akdogan, Y. A., Cingoz, A., & Akabali, O. A. (2021). Determination and validation of the Turkish Geoid Model-2020 (TG-20). *Bulletin of Geophysics and Oceanography*, *62*(3), 495–512. https://doi.org/10.4430/bgta0345